Fly 8:2, 113–119; April/May/June 2014; © 2014 Landes Bioscience

Germline and somatic vitelline proteins colocalize in aggregates in the follicular epithelium of *Drosophila* ovaries

Marc Furriols[1,2,*] and Jordi Casanova[1,2,*]

[1]Institut de Biologia Molecular de Barcelona (IBMB-CSIC); Barcelona, Catalonia, Spain; [2]Institute for Research in Biomedicine (IRB Barcelona); Barcelona, Catalonia, Spain

Keywords: Nasrat, Polehole, CVM32E, SV23, follicle cells

Nasrat and Polehole, two *Drosophila* proteins related functionally and by sequence, are secreted from the oocyte and incorporated into the vitelline membrane, where they play a role in the integrity of the same and in the activation of embryonic Torso RTK. In addition, they also accumulate in a punctate pattern in the follicular epithelium. Here we show that their accumulation at the follicle cells depends on their gene expression in the germline, indicating that these proteins move from the oocyte to the follicle cells in a process that does not require endocytosis. Finally we used cell markers to examine the distribution of these proteins at the follicle cells and show they accumulated in aggregates with vitelline membrane proteins in close association with the plasmatic membrane. We propose that these aggregates represent spatially restricted sinks for vitelline membrane proteins that fail to be incorporated into vitelline bodies and later on into the vitelline membrane.

Introduction

The *Drosophila* eggshell is a specialized ECM that surrounds and protects the embryo until its eclosion. Synthesized by the somatic follicle cells surrounding the oocyte, the eggshell consists of five morphologically distinct layers, the vitelline membrane being the layer closest to the oocyte.[1,2]

The vitelline membrane is the first layer to be synthesized, a process that occurs from stage 8 to stage 10 of oogenesis.[3] During stage 9, follicle cells begin to secrete vitelline membrane proteins, which aggregate in the perivitelline space in vesicles called "vitelline bodies." These structures are physically separated by microvilli that extend from the oocyte and follicle cells, spanning the perivitelline space.[4] By stage 10B of oogenesis, the microvilli shorten and the vitelline bodies fuse to form a 1.7-mm thick continuous layer over the entire oocyte, which gradually thins to a thickness of 0.3 mm as oogenesis proceeds.[1,5]

Although the vitelline membrane was originally thought to comprise proteins secreted only by follicle cells, we recently showed that this structure also receives contributions from the oocyte.[6] On the one hand, four major structural proteins of the vitelline membrane are secreted by follicle cells (sV17, sV23, Vm32E, and Vm34C).[2,3,7,8] The assembly of these proteins into the membrane requires their stage-specific proteolytic processing and cross-linking to render the membrane insoluble.[2,5,7] On the other hand, *fs(1)Nasrat* (*fs(1)N*), *fs(1)polehole* (*fs(1)ph*), and *closca* (*clos*) encode a group of proteins secreted from the oocyte, coating the oocyte surface in a finger-like pattern, as detected by whole-mount immuno-fluorescence.[6,9] A more precise characterization by immuno-electron microscopy shows the accumulation of Nasrat at the vitelline bodies and the vitelline membrane.[6] Nasrat, Polehole, and Closca are related by sequence and function and play a dual role, being involved in vitelline membrane integrity and in the specification of the terminal regions of the embryo; furthermore, they are mutually required for extracellular accumulation.[6,9-11]

In addition to their accumulation at the periphery of the oocyte, Nasrat and Polehole are detected in a punctate pattern in follicle cells.[9] While it has not been possible to observe a similar pattern for Closca with either a HA-tagged construct or an antibody against the protein, Polehole fails to accumulate in the follicle cells of *clos* null mutant egg chambers, thus arguing for a similar accumulation of Closca in these cells, albeit under the detection threshold.[6] Here we characterized the accumulation of Polehole and Nasrat in the follicular epithelium cells and show that their accumulation at the follicle cells depends on *fs(1)Nasrat* and *fs(1)polehole* germline expression, indicating that these proteins move from the oocyte to the follicle cells. We also show that this accumulation corresponds to multiproteic aggregates of vitelline membrane proteins from both the oocyte and the follicle cells associated with the cell membranes. We propose that these aggregates serve as sink deposits for vitelline proteins present in excess.

*Correspondence to: Marc Furriols; Email: mfebmc@ibmb.csic.es; Jordi Casanova; Email: jcrbmc@ibmb.csic.es
Submitted: 04/01/2014; Revised: 04/29/2014; Accepted: 05/06/2014; Published Online: 05/09/2014
http://dx.doi.org/10.4161/fly.29133

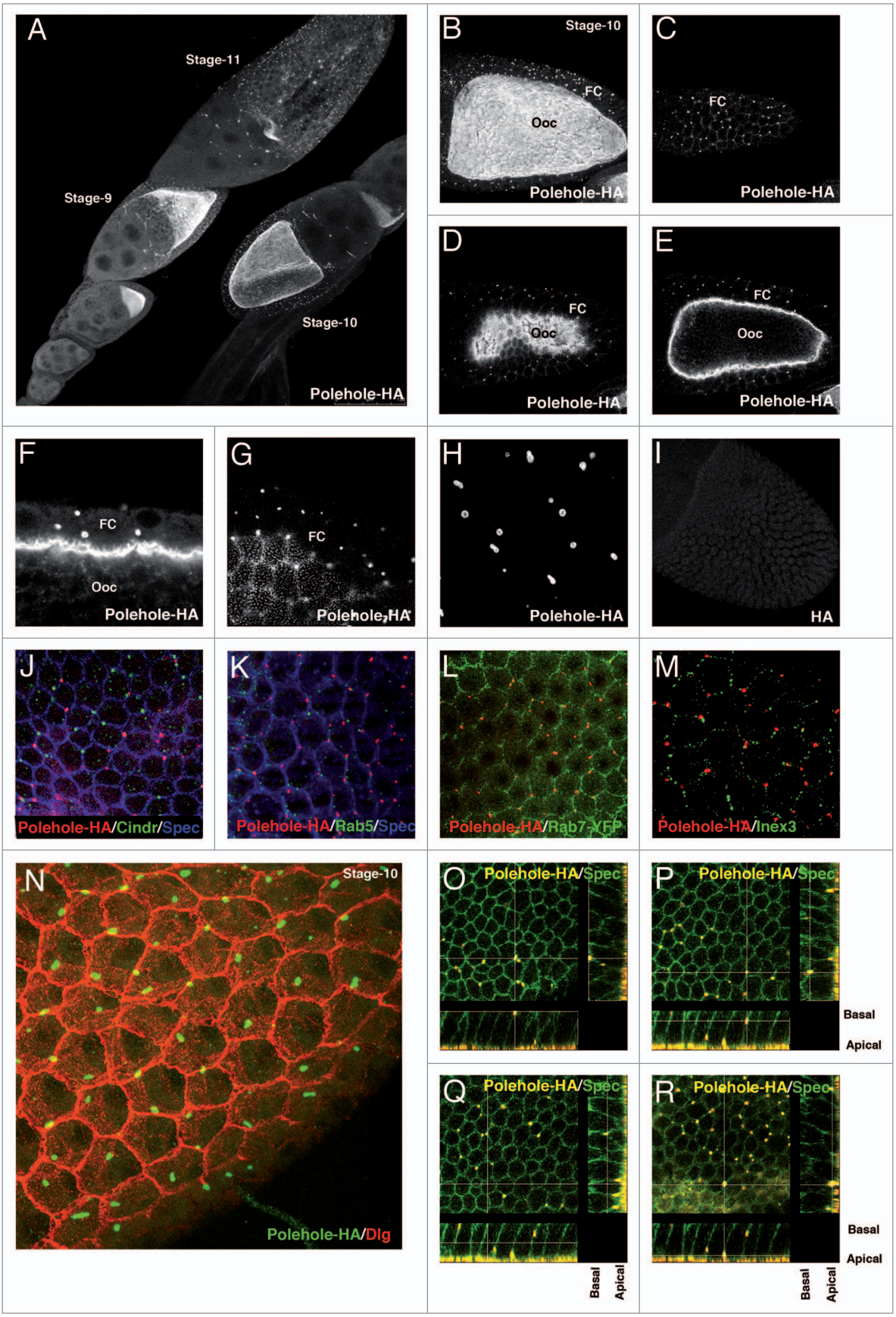

Figure 1. For figure legend, see page 108.

Results and Discussion

Polehole accumulates in puncta at the follicle cells associated with the plasmatic membrane

The distribution of Polehole and Nasrat can be detected by means of HA-tagged constructs that rescue the sterility of females homozygous for *fs(1)ph*^{1901} and *fs(1)N*^{211} respectively.[9] While Polehole accumulates in a finger-like pattern mainly at the oocyte periphery, it is also detected in a punctate pattern at the somatic follicle cells surrounding the oocyte (ref. 9; **Fig. 1A–I**). Polehole accumulation in the follicular epithelium was first detected at late stage 9 of oogenesis (**Fig. 1A**) and persisted until stage 13 or even stage 14 (data not shown). Higher magnification revealed that the Polehole puncta were circular (**Fig. 1H**).

To further characterize the accumulation of Polehole at the follicle cells, we studied whether they overlap with specific markers with similar patterns. The shape of Nasrat and Polehole puncta (**Fig. 1H**) first suggested that they corresponded to follicle ring canals.[9] However, the aggregates of these two proteins did not colocalize with those of GFP::Pav-KLP, a ring canal marker.[12] In agreement with this observation, neither did we detect the colocalization of Polehole with Cindr (**Fig. 1J**), the *Drosophila* CD2AP/CIN85 ortholog and a component of somatic ring canals.[13] Likewise, Polehole puncta did not overlap with endosome markers such as Rab5 and Rab7[14] (**Fig. 1K–L**) or gap junction markers such as Inex3[15] (**Fig. 1M**). However, we found a close association of Polehole puncta with the plasmatic membrane of follicle cells (**Fig. 1N–R**). This association was detected along the entire apicobasal axis (**Fig. 1O–R**), although the puncta most often were located at the vertices where three cells came together (**Fig. 1O–R**).

Polehole accumulates in aggregates with vitelline membrane proteins

Analysis of the vitelline membrane protein VM32E showed a similar punctate accumulation at the follicle cells. At stage 10 of oogenesis, VM32E is synthesized in follicle cells and detected in small dots in the same (**Fig. 2A, C, D, and F**; ref. 16) and in the perivitelline space, where the vitelline membrane forms (**Fig. 2A and C**;ref. 16). In addition, VM32E was also detected in larger puncta (**Fig. 2D and F**), which were more evident from stage 11 (**Fig. 2G and I**) till late stages of oogenesis (**Fig. 5J and L**). Interestingly, there was a considerable overlap between the large VM32E puncta and Polehole punta (**Fig. 2D, E, G, H, J, and K**). This is not a specific feature of VM32E as another vitelline membrane protein, sV23,[7] also accumulates in puncta at the follicle cells, similarly colocalizing with Polehole (**Fig. 2M–O**).

However, and conversely to the mutual requirement of Nasrat and Polehole, vitelline membrane proteins do not require any of these two proteins for their accumulation at the follicle cells. Similarly Nasrat and Polehole do not require the vitelline membrane proteins for their accumulation at the follicle cells. Thus, VM32E puncta are detected at the the follicle cells of *fs(1)N*^{14} mutant egg chambers (**Fig. 3A–D**), and Polehole puncta at the follicle cells of egg chambers mutant for the gene encoding sV23 (*VM26Ab*^{QJ42}, see Experimental Procedures), (**Fig. 3E and F**). We could not test the requirement of VM32 genetically as there are no mutants for this vitelline protein; however, *VM32E* is not expressed in the most posterior follicle cells of stage 10 egg chambers[16] and, nevertheless, Polehole puncta are detected at these posterior follicle cells (**Fig. 3G and H**).

Accumulation of Nasrat in the follicular epithelium depends on fs(1)Nasrat germline expression

Accumulation of Nasrat and Polehole at the follicle cells may arise either from undetectable *fs(1)N* and *fs(1)ph* expression in these cells or from the internalisation of these two proteins from the perivitelline space.[9] Since both proteins are detected by HA-constructs and no antibodies are available against either, we could not address the origin of their accumulation at the follicle cells by antibody detection. However, we took advantage of the fact of the mutual extracellular dependence of Nasrat and Polehole.[9] We thus generated clones for the null allele *fs(1)N*^{14} and examined the accumulation of Polehole-HA in these ovaries. Polehole was absent in the follicular epithelium of *fs(1)N*^{14} germline clones (**Fig. 4C and D**) but was present in the follicular epithelium of *fs(1)N*^{14} somatic clones (**Fig. 4E and E'**). Since Nasrat is required for the extracellular accumulation of Polehole,[9] these results indicate that Nasrat accumulation in the follicular epithelium depends on *fs(1)N* germline expression and, moreover, that Nasrat moves from the oocyte to the follicle cells.

How are these aggregates generated at the follicle cells? One possibility is that secreted Polehole in the perivitelline space is internalised into these cells by endocytosis and then transported to lateral membranes. To test this hypothesis, we characterized the accumulation of Polehole in somatic clones of Rab5^{DN} and Shibire (shi)^{DN}, in which endocytosis is impaired.[17,18] The accumulation of Polehole was not compromised in follicle cell flip-out clones of either Rab5^{DN} or Shi^{DN} (**Fig. 5A–C and 5D–F**, respectively), thereby suggesting that endocytosis is not required for Polehole

Figure 1. Polehole accumulates in follicle cells in a punctate pattern associated with the plasmatic membrane. In all figures Polehole is shown as detected with an anti-HA antibody (3F10) in *fs(1)ph-HA* transgenic egg chambers. (**A**) Projection of confocal sections from egg chambers at various stages of oogenesis. Punctate accumulation of Polehole in the follicular epithelium is detected from late stage 9 until late oogenesis. (**B**) Projection of confocal sections from a stage 10 egg chamber. (**C–E**) Different confocal sections from the egg chamber in B; Polehole is detected in puncta in follicle cells and at the oocyte surface. (**F–G**) Magnifications of the same egg chamber show the finger-like accumulation pattern on the oocyte surface. (**H**) A higher magnification view show the circular shape of the Polehole puncta. (**I**) Projection of confocal sections from a wild-type stage 10 egg chamber stained with an anti-HA antibody (3F10) to show that the follicle cell puncta detected in *fs(1)ph-HA* transgenic egg chambers are specific. (**J–M**) Projection of superficial confocal sections from stage 10 egg chambers to show lack of colocalization between Polehole (in red) and the somatic intercellular bridge marker Cindr (in green in J), the early endosome marker Rab5 (in green in K), the late endosome marker Rab7-YFP (in green in L), and the gap junction marker Inexin3 (in green in M). (**N**) Projection of superficial confocal sections from a stage 10 egg chamber shows Polehole puncta (in green) associated with follicle cell membranes, as detected with anti-Discs large antibody (in red). (**O–R**) Superficial confocal sections from a stage 10 egg chamber with their corresponding Z-projections from basal to apical to show Polehole aggregates (in red) at all positions along the apicobasal axis at the cell membrane, detected with an anti-Spectrin antibody (in green). Ooc, oocyte. FC, follicle cells.

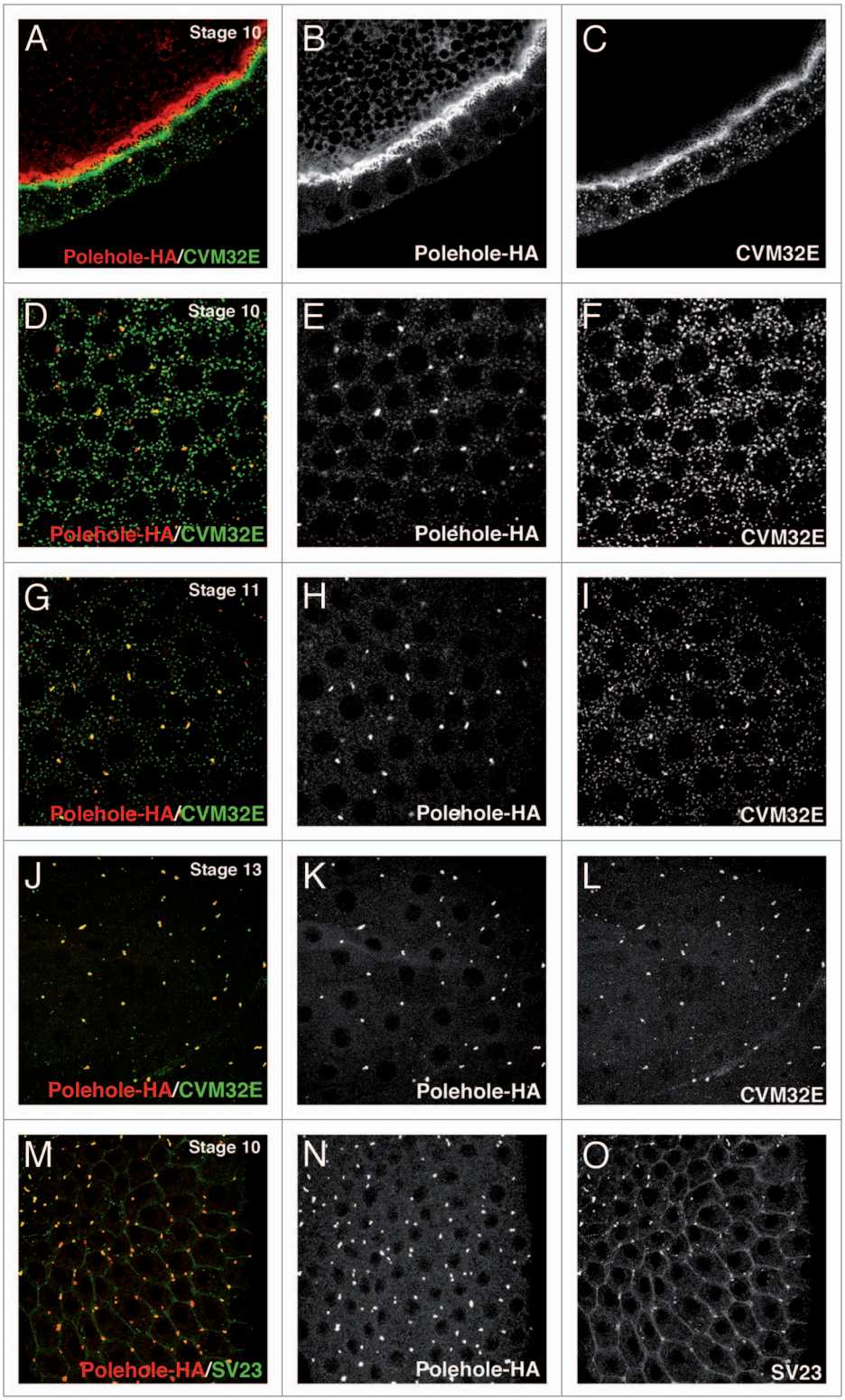

Figure 2. Polehole accumulates in aggregates with vitelline membrane proteins. (**A**) Internal confocal section from a stage 10 egg chamber to show Polehole (in red) and CVM32E (in green). Polehole and CVM32E are detected in the perivitelline space in complementary finger-like patterns. In follicle cells CVM32E is also detected in small puncta in the cytoplasm and in larger ones overlapping with Polehole. (**B and C**) Single channels of panel A. (**D–L**) Projections of superficial confocal sections and single channel panels of stage 10 (**D–F**), stage 11 (**G–I**) and stage 13 (**J–L**) egg chambers show colocalization at large puncta of Polehole (in red) and CVM32E (in green) (**M–O**) Similar views from a stage 10 egg chamber showing accumulation of Polehole (in red) and sV23 (in green).

accumulation at the follicle cells. These results are consistent with the absence of colocalization between Polehole and the endosomal markers. Alternatively, the follicular accumulation of Polehole may arise by transport between the oocyte and follicle cells through gap junctions or by diffusion of secreted Polehole in the perivitelline space between the lateral membranes of the follicle cells. Although the oocyte and ovarian follicle cells are connected by gap junctions,[15] the possibility that Polehole and Nasrat are transported into these cells through gap junctions is unlikely because these proteins are much larger than the maximum size estimated for a molecule to be exchanged by arthropod gap junctions.[19-21] We favor the diffusion scenario because, at vitellogenic stages 9 and 10 of oogenesis, there is a transient loosening of the follicular cell layer that allows the hemolymph carrying the yolk protein precursors to reach the oocyte membrane, where these precursors are subsequently taken up into the oocyte by endocytic vesicles.[4,22] Therefore, free Polehole secreted from the oocyte could diffuse in the enlarged interfollicular spaces between the lateral membranes of the follicle cells to end up forming aggregates with the vitelline membrane proteins synthesized by the follicle cells. A similar mechanism could account for the contribution of vitelline membrane proteins secreted by follicle cells to the aggregates, as no exocytosis has been observed laterally at the enlarged interfollicular spaces.[4] Interestingly, these aggregates are reminiscent of the pattern of accumulation of the endosymbiotic bacteria *Spiroplasma poulsonii* detected between the follicle cells as they travel from the hemolymph into the oocyte.[23]

We examined whether Nasrat, Polehole and Closca have a specific role in the follicular epithelium. However, we did not detect any obvious defect in follicle cell morphology, polyploidy of follicle cell nuclei, vitelline membrane protein secretion, chorion morphology, or chorion gene amplification in *fs(1)* N^{14} mutant egg chambers (data not shown). All together, these results suggest that the aggregates at the follicle cells represent spatially restricted sinks

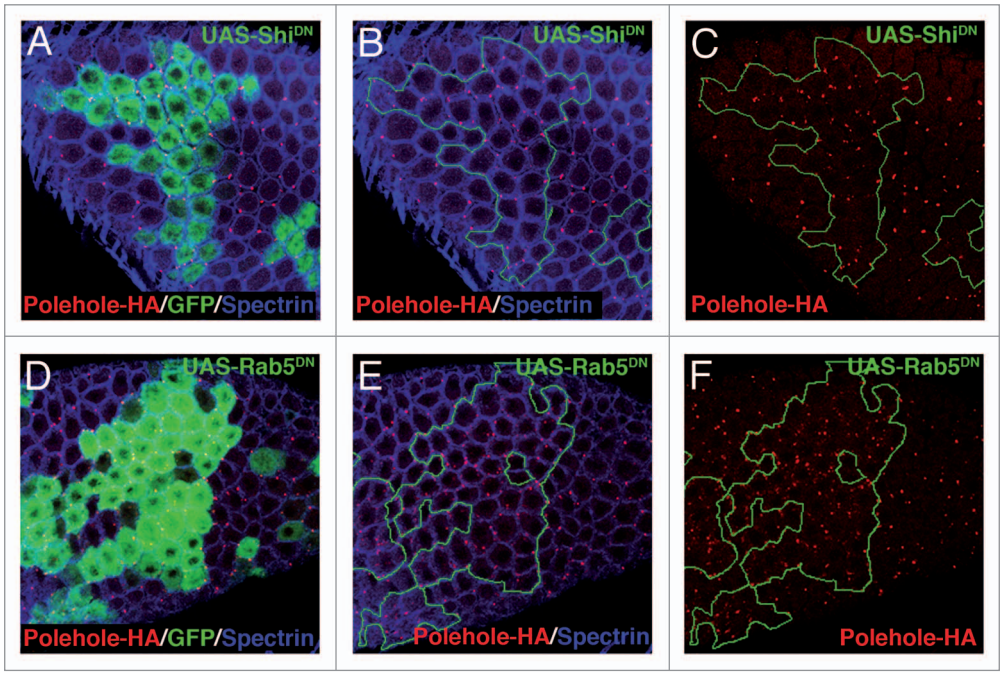

Figure 5. Accumulation of Polehole in follicle cells is not impaired by the downregulation of endocytosis. Projection of superficial confocal sections from stage 10 egg chambers with either Shibire^{DN} (**A–C**) or Rab5^{DN} (**D–F**) flip-out clones detected by GFP (in green) show normal accumulation of Polehole (in red) in the mutant follicle cells (outlined). Cell membranes are detected in some panels by an anti-Spectrin antibody (in blue).

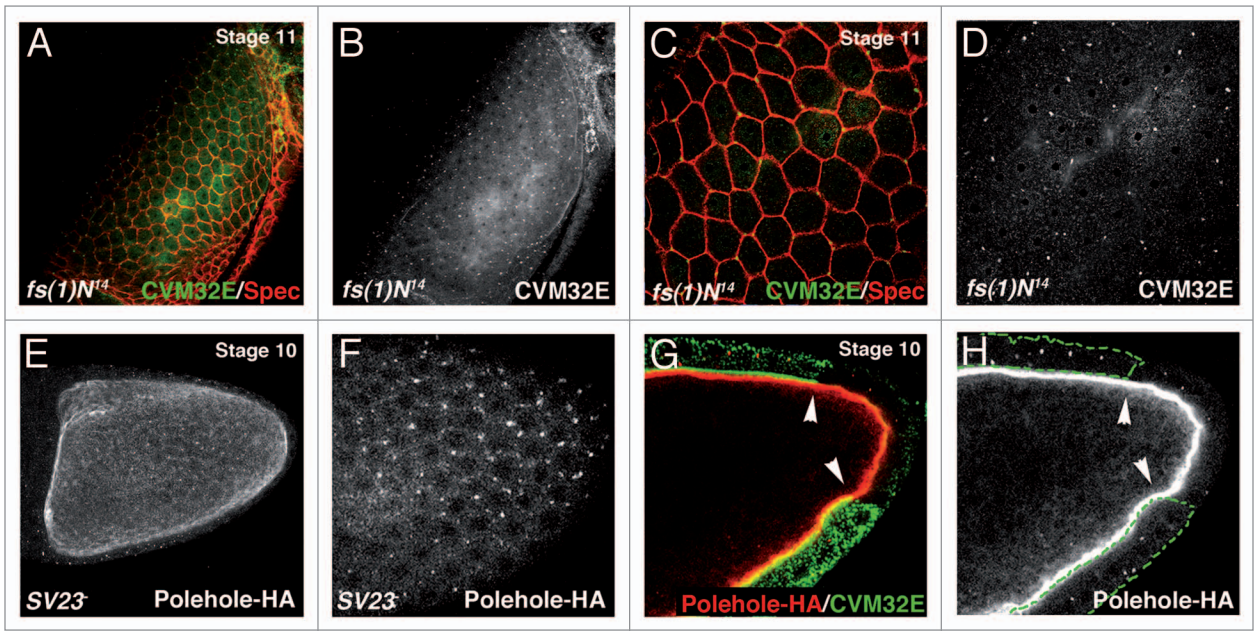

Figure 3. Independent accumulation of Polehole and vitelline membrane proteins in follicle cell aggregates. (**A**) Projection of confocal sections from a stage 10 fs(1)*N*^{14} egg chamber to show normal VM32E puncta (in green) associated with the plasmatic membrane of follicle cells, as visualized by anti-Spectrin antibody (in red). (**B**) Single channel of panel A. (**C**) Magnification of the picture in panel A. (**D**) Single channel of panel C. (**E**) Projection of confocal sections from a stage 10 egg chamber mutant for the gene encoding sV23 protein to show normal Polehole accumulation. (**F**) A magnification of the picture in panel E to show Polehole puncta. (**G**) Confocal section from a stage 10 egg chamber to show Polehole (in red) and CVM32E (green) accumulation; Polehole puncta are also detected in the most posterior follicle cells, where CVM32E is not present at this stage (borders indicated by white arrowheads). (**H**) Single channel of panel G.

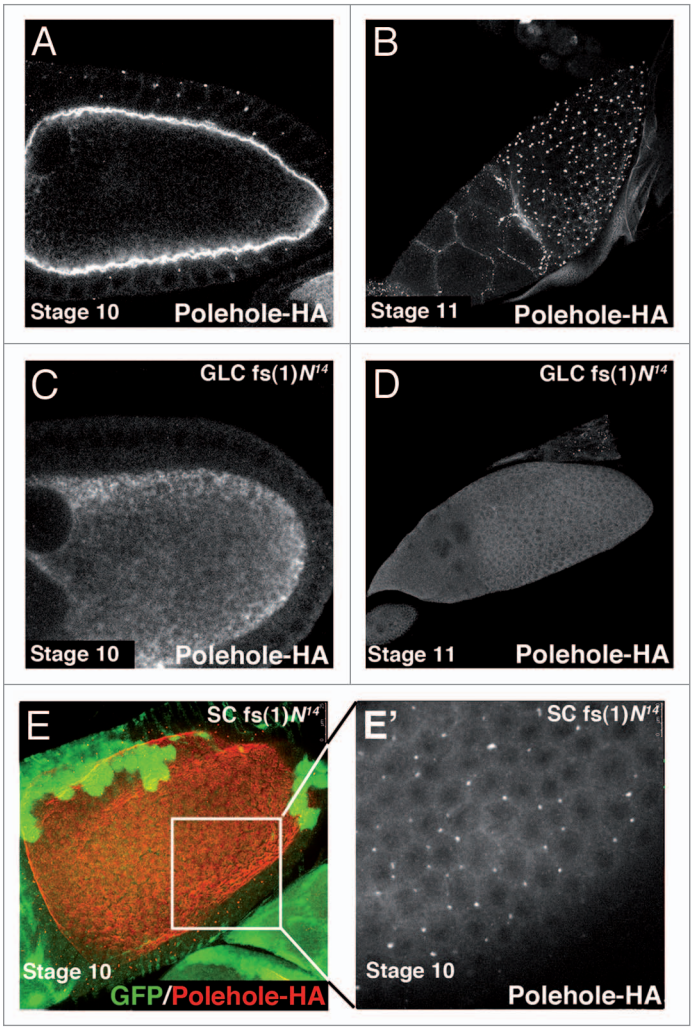

Figure 4. Accumulation of Polehole in follicle cells depends on *fs(1)N* germline expression. (**A and B**) Confocal section from a stage 10 egg chamber (A) and projection of confocal sections from a stage 11 egg chamber (B) to show Polehole accumulation. (**C and D**) Confocal section from a stage 10 egg chamber (C) and projection of confocal sections from a stage 11 egg chamber with a $fs(1)N^{14}$ germline clone (GLC) do not show Polehole accumulation at the oocyte surface or in the follicle cell punctae. (**E**) Projection of confocal sections from a stage 10 egg chamber with a $fs(1)N^{14}$ somatic clone (SC), detected by the lack of GFP (in green), shows normal Polehole accumulation (in red). (**E'**) A single channel magnification of the most superficial confocal sections of the picture in (E) to show normal Polehole puncta in the $fs(1)N^{14}$ mutant follicle cells .

for vitelline membrane proteins secreted in excess into the perivitelline space or that fail to be incorporated into vitelline bodies and later on into the vitelline membrane.

Materials and Methods

Drosophila stocks and genetics

We used the following *Drosophila* stocks described in Flybase (http://flybase.bio.indiana.edu): *fs(1)ph-HA* (FBal0135724), $fs(1)N^{14}$ (FBal0135717), *FRT101* (FBti0002055), *FRT101 GFP*, *FRT101 OvoD* (FBal0013375), *hs-FLP-38* (FBti0002054), $UAS\text{-}Shi^{K44A}3.10$ (FBti0015791),[18] $UAS\text{-}DRab5^{S43N}$ (FBti0150350),[17] *UAS-CD8-GFP*, *Tub* > $y{+}GAl^{80}$ > *Gal4* and *Rab7-YFP* (FBal0215398). The combination $VM26Ab^{QJ42}$ (FBal0018017)/*Def BSC183* (FBab0045073) was used as mutant condition for the gene encoding sV23 vitelline membrane protein.[24] We performed the following clonal analyses: (1) For $fs(1)N^{14}$ germline clones, late third instar larvae of the genotype *FRT101* $fs(1)N^{14}$/ *FRT101 OvoD*; *fs(1)ph-HA*/hs-FLP-38 were heat-shocked twice for 1 h at 37 °C, with a 2 h interval; (2) For $fs(1)N^{14}$ somatic clones, females of the genotype *FRT101* $fs(1)N^{14}$/ *FRT101 GFP*; *fs(1)ph-HA*/*hs-FLP-38* were heat-shocked twice for 1h at 37 °C, with a 2 h interval, during 3 consecutive days, and ovaries were dissected 4–6 d after the last heat-shock; (3) For flip-out clones, females of the genotype *hs-FLP*/+; *UAS-CD8-GFP*/*fs(1)ph-HA*; *Tub* > $y{+}GAl^{80}$ > *Gal4*/ $UAS\text{-}Shi^{K44A}3.10$ or *hs-FLP*/+; *UAS-CD8-GFP*/*fs(1)ph-HA*; *Tub* > $y{+}GAl^{80}$ > *Gal4*/$UAS\text{-}DRab5^{S43N}$ were heat-shocked at 37 °C for 1 h, and ovaries were dissected 24 h after the heat-shock; under these conditions, flip-out clones analyzed at stage 10B were generated at late stage 7.

Antibody staining

Females were placed in fly food vials supplemented with fresh yeast paste 1–2 d before dissection. Ovaries were dissected in cold PBS, fixed for 20 min in 4% formaldehyde with PBS 0.1% Triton X-100 (PBT), rinsed 3–5x with PBT, blocked for 1 h with PBT 10%BSA, and incubated overnight with the primary antibodies in PBT 1%BSA. They were then washed for 1–2 h with PBT 1%BSA (changed every 20–30 min) and incubated 2–4 h with the secondary antibodies in PBT 0.1%BSA, washed for 10 min 3x with PBT and mounted in nPG antifade mounting media (glycerol 80% n-propyl-gallate 0.4%). As indicated in Haglund et al. (2010), ovaries were fixed on ice for 25 min when anti-Cindr antibody was used. The following primary antibodies were used: rat monoclonal anti-HA 1/300 (3F10, Roche), mouse anti-Dlg 1/500 (4F3, Developmental Studies Hybridoma Bank), rat monoclonal anti-Spectrin 1/5 (3A9, Developmental Studies Hybridoma Bank), goat anti-GFP 1/300 (6673, Abcam), rabbit anti-GFP 1/300 (A11122, Invitrogen), purified rabbit anti-Cindr 1/500,[13] rabbit anti-Rab5 1/1000 (Abcam, ab31261), guinea pig anti-Inex3 1/20,[15] rabbit anti-CVM32E 1/100,[16] rabbit anti-sV23 1/250.[7] Secondary antibodies were used at 1/300 (Jackson ImmunoResearch). Confocal images were obtained with a Leica SPE. Images were assembled with Adobe Photoshop.

Disclosure of Potential Conflicts of Interest

No potential conflicts of interest were disclosed.

Acknowledgments

We thank R. Bauer, I. Becam, S. Eaton, G. Gargiulo, M.González-Gaitan, K. Haglund, A. Kramerov, M. Milan, G. Waring, the Bloomington Drosophila Stock Center, and the Developmental Studies Hybridoma Bank for flies and reagents; E. Fuentes, N. Martin, and Y. Rivera for technical assistance; T. Yates for help with preparing the manuscript; colleagues in the lab for discussions and A. Casali and A. Mineo for comments on the manuscript.

References

1. Margaritis LH, Kafatos FC, Petri WH. The eggshell of Drosophila melanogaster. I. Fine structure of the layers and regions of the wild-type eggshell. J Cell Sci 1980; 43:1-35; PMID:6774986
2. Waring GL. Morphogenesis of the eggshell in Drosophila. Int Rev Cytol 2000; 198:67-108; PMID:10804461; http://dx.doi.org/10.1016/S0074-7696(00)98003-3
3. Cavaliere V, Bernardi F, Romani P, Duchi S, Gargiulo G. Building up the Drosophila eggshell: first of all the eggshell genes must be transcribed. Dev Dyn 2008; 237:2061-72; PMID:18651659; http://dx.doi.org/10.1002/dvdy.21625
4. Trougakos IP, Papassideri IS, Waring GL, Margaritis LH. Differential sorting of constitutively co-secreted proteins in the ovarian follicle cells of Drosophila. Eur J Cell Biol 2001; 80:271-84; PMID:11370742; http://dx.doi.org/10.1078/0171-9335-00163
5. Margaritis LH. The egg-shell of Drosophila melanogaster III. Covalent crosslinking of the chorion proteins involves endogenous hydrogen peroxide. Tissue Cell 1985; 17:553-9; PMID:18620142; http://dx.doi.org/10.1016/0040-8166(85)90031-X
6. Ventura G, Furriols M, Martín N, Barbosa V, Casanova J. closca, a new gene required for both Torso RTK activation and vitelline membrane integrity. Germline proteins contribute to Drosophila eggshell composition. Dev Biol 2010; 344:224-32; PMID:20457146; http://dx.doi.org/10.1016/j.ydbio.2010.05.002
7. Pascucci T, Perrino J, Mahowald AP, Waring GL. Eggshell assembly in Drosophila: processing and localization of vitelline membrane and chorion proteins. Dev Biol 1996; 177:590-8; PMID:8806834; http://dx.doi.org/10.1006/dbio.1996.0188
8. Andrenacci D, Cernilogar FM, Taddel C, Rotoli D, Cavaliere V, Graziani F, Gargiulo G. Specific domains drive VM32E protein distribution and integration in Drosophila eggshell layers. J Cell Sci 2001; 114:2819-29; PMID:11683415
9. Jiménez G, González-Reyes A, Casanova J. Cell surface proteins Nasrat and Polehole stabilize the Torso-like extracellular determinant in Drosophila oogenesis. Genes Dev 2002; 16:913-8; PMID:11959840; http://dx.doi.org/10.1101/gad.223902
10. Degelmann A, Hardy PA, Mahowald AP. Genetic analysis of two female-sterile loci affecting eggshell integrity and embryonic pattern formation in Drosophila melanogaster. Genetics 1990; 126:427-34; PMID:2123163
11. Cernilogar FM, Fabbri F, Andrenacci D, Taddei C, Gargiulo G. Drosophila vitelline membrane cross-linking requires the fs(1)Nasrat, fs(1)polehole and chorion genes activities. Dev Genes Evol 2001; 211:573-80; PMID:11819114; http://dx.doi.org/10.1007/s00427-001-0192-1
12. Airoldi SJ, McLean PF, Shimada Y, Cooley L. Intercellular protein movement in syncytial Drosophila follicle cells. J Cell Sci 2011; 124:4077-86; PMID:22135360; http://dx.doi.org/10.1242/jcs.090456
13. Haglund K, Nezis IP, Lemus D, Grabbe C, Wesche J, Liestøl K, Dikic I, Palmer R, Stenmark H. Cindr interacts with anillin to control cytokinesis in Drosophila melanogaster. Curr Biol 2010; 20:944-50; PMID:20451383; http://dx.doi.org/10.1016/j.cub.2010.03.068
14. Marois E, Mahmoud A, Eaton S. The endocytic pathway and formation of the Wingless morphogen gradient. Development 2006; 133:307-17; PMID:16354714; http://dx.doi.org/10.1242/dev.02197
15. Bohrmann J, Zimmermann J. Gap junctions in the ovary of Drosophila melanogaster: localization of innexins 1, 2, 3 and 4 and evidence for intercellular communication via innexin-2 containing channels. BMC Dev Biol 2008; 8:111; PMID:19038051; http://dx.doi.org/10.1186/1471-213X-8-111
16. Andrenacci D, Cavaliere V, Cernilogar FM, Gargiulo G. Spatial activation and repression of the drosophila vitelline membrane gene VM32E are switched by a complex cis-regulatory system. Dev Dyn 2000; 218:499-506; PMID:10878615; http://dx.doi.org/10.1002/1097-0177(200007)218:3<499::AID-DVDY1006>3.0.CO;2-J
17. Entchev EV, Schwabedissen A, González-Gaitán M. Gradient formation of the TGF-beta homolog Dpp. Cell 2000; 103:981-91; PMID:11136982; http://dx.doi.org/10.1016/S0092-8674(00)00200-2
18. Moline MM, Southern C, Bejsovec A. Directionality of wingless protein transport influences epidermal patterning in the Drosophila embryo. Development 1999; 126:4375-84; PMID:10477304
19. Berdan RC. Intercellular communication in arthropods: Biophysical, ultrastructural and biochemical approaches. In: DeMello eWC, ed. Cell-to-Cell Communication Plenum Press, 1987: pp. 299-370.
20. Waksmonski SL, Woodruff RI. For uptake of yolk precursors, epithelial cell-oocyte gap junctional communication is required by insects representing six different orders. J Insect Physiol 2002; 48:667-75; PMID:12770077; http://dx.doi.org/10.1016/S0022-1910(02)00095-1
21. Brooks RA, Woodruff RI. Calmodulin transmitted through gap junctions stimulates endocytic incorporation of yolk precursors in insect oocytes. Dev Biol 2004; 271:339-49; PMID:15223338; http://dx.doi.org/10.1016/j.ydbio.2004.03.037
22. DiMario PJ, Mahowald AP. Female sterile (1) yolkless: a recessive female sterile mutation in Drosophila melanogaster with depressed numbers of coated pits and coated vesicles within the developing oocytes. J Cell Biol 1987; 105:199-206; PMID:2886508; http://dx.doi.org/10.1083/jcb.105.1.199
23. Herren JK, Paredes JC, Schüpfer F, Lemaitre B. Vertical transmission of a Drosophila endosymbiont via cooption of the yolk transport and internalization machinery. MBio 2013; 4:4; PMID:23462112; http://dx.doi.org/10.1128/mBio.00532-12
24. Savant SS, Waring GL. Molecular analysis and rescue of a vitelline membrane mutant in Drosophila. Dev Biol 1989; 135:43-52; PMID:2504634; http://dx.doi.org/10.1016/0012-1606(89)90156-5